KI REPORTS
KIReports.org
TRANSLATIONAL RESEARCH

Gene Expression Sets and Renal Profiling from the Renal AL Amyloid Involvement and NEOD00 (RAIN) Trial

Cindy Varga[1], Felix Eichinger[2], Viji Nair[2], Abhijit S. Naik[2], Samih H. Nasr[3], Agnes B. Fogo[4], Denis Toskic[5], Matthias Kretzler[2] and Raymond L. Comenzo[5]

[1]Plasma Cell Disorders Division, Atrium Health Levine Cancer Institute, Charlotte, North Carolina, USA; [2]Division of Nephrology, University of Michigan, Ann Arbor, Michigan, USA; [3]Department of Laboratory Medicine and Pathology, Mayo Clinic, Rochester, Minnesota, USA; [4]Department of Pathology, Microbiology and Immunology, Vanderbilt University Medical Center, Nashville, Tennessee, USA; and [5]Tufts University School of Medicine, John C. Davis Myeloma and Amyloid Program, Tufts Medical Center, Boston, Massachusetts, USA

Introduction: There is an unmet need to understand the mechanisms by which amyloid deposition drives alterations in the kidney. We leveraged renal biopsies from amyloid light-chain (AL) amyloidosis participants of the Renal AL Amyloid Involvement and NEOD00 (RAIN) trial (NCT03168906) to perform transcriptional profiling and to employ a novel histologic scoring tool. Our objective was to utilize a transcriptome-driven approach to identify AL molecular signatures that may be prognostic.

Methods: Clinical data were correlated to histologic and molecular findings. A composite scarring injury and amyloid score (AS) were assigned to each biopsy. Glomerular and tubulointerstitial (TI) compartments were microdissected and sequenced separately. Expression data were compared to healthy living donors and focal segmental glomerulosclerosis (FSGS) profiles. Differentially expressed genes were determined.

Results: Cluster analysis revealed 2 distinct patient clusters (G1 and G2) based on gene expression. The AS was higher in the TI compartment (6.5 vs. 4.5; $P = 0.0290$) of G2. Glomeruli showed activation of fibrotic pathways and increased canonical signaling of LPS/IL-1. TNF activation was noted in TI. Enriched ingenuity canonical pathways included "coagulation system," "GADD45 signaling," and "Wnt/Ca+ pathway," among others. For AL versus living donors, ingenuity pathway analysis identified enrichment in PI3K/Akt signaling. Gene regulators of cellular proliferation were enriched in the amyloid group.

Conclusion: Despite the small sample size, we identified 2 distinct groups of patients with AL based on molecular signatures. Detailed studies of a larger cohort encompassing omics technologies at a single cell resolution will further help to identify the response of individual kidney cell types to amyloid deposits, potentially leading to the development of novel therapeutic targets.

Kidney Int Rep (2024) **9,** 2786–2797; https://doi.org/10.1016/j.ekir.2024.07.002
KEYWORDS: AL amyloidosis; proteinuria; transcriptional profiling

Amyloid light-chain (AL) amyloidosis is an orphan disease in which clonal plasma cells produce serum-free light chains (lambda or kappa) that misfold and deposit in and around soft tissue and organs. More than 70% of patients present with renal dysfunction at diagnosis.[1-3] Without intervention, the kidneys rapidly deteriorate within 1 to 2 years, and these patients, who are seldom eligible for kidney transplants, ultimately require dialysis until their early death. Successful therapy in AL is characterized by achieving a complete hematologic response to chemotherapy, which is defined by normalizing the kappa to lambda ratio and the disappearance of the monoclonal protein in the serum and urine.[3] A renal response is a >30% decline in proteinuria or a decrease of proteinuria below 500 mg in 24 hours without a >25% estimated glomerular filtration rate (eGFR) decrease.[4] Although a complete response has been associated with prolonged overall survival and a 68% reduction in renal progression,[5,6] as many as 30% of patients will eventually progress to end-stage renal disease while in a maintained hematologic response.[7]

The mechanism by which amyloid deposits result in cellular injury, tissue damage, and organ dysfunction is incompletely understood. The deduction that organ dysfunction results from amyloid replacement of parenchymal tissue is oversimplified. A better

Correspondence: Cindy Varga, Levine Cancer Institute, 1021 Morehead Medical Dr, Charlotte, North Carolina 28204-2990, USA. E-mail: cindy.varga@atriumhealth.org

Received 17 June 2024; accepted 2 July 2024; published online 11 July 2024

understanding of the molecular mechanisms underlying renal damage in AL amyloidosis is needed to stratify these patients better and unveil potential therapeutic targets to improve patient outcomes.

The RAIN trial (NCT03168906) was a phase 2b multicenter study that evaluated the safety and efficacy of NEOD001, a monoclonal antibody thought to bind to amyloid fibrils,[8] in patients with known renal amyloidosis. All participants underwent a renal biopsy prior to drug randomization. Unfortunately, the RAIN trial was prematurely closed based on results from a phase 2b study and a futility analysis of a phase 3 study utilizing NEOD001. By the time RAIN was closed, there were 9 evaluable patients enrolled. However, the data we obtained from these patients' kidney biopsies are invaluable. We leveraged tissue from these biopsies to perform gene expression profiling in collaboration with the University of Michigan. We also implemented a novel histologic scoring system with 2 expert renal pathologists. Herein, we present the significant findings from these ancillary studies.

METHODS

Trial Design and Study Population

The RAIN study was a phase 2b, multicenter, double-blind, safety and efficacy study of NEOD001 enrolling patients from April 12, 2017, through April 23, 2018, at 3 sites in the United States (Tufts Medical Center, University of California San Francisco, and Karmanos Cancer Institute Wayne State University). The institutional review board or independent ethics committee at each study center approved the protocol, and the study was performed following the International Conference on Harmonization Good Clinical Practice guidelines and the principles of the Declaration of Helsinki. The study was designed by the sponsor (Tufts Medical Center). The study schema is presented in Supplementary Figure S1. Patients were previously treated with antiplasma cell therapy and had persistent proteinuria (>500 mg/d; predominantly albumin) despite maintaining at least a stable partial hematologic response to the most recent antiplasma cell therapy. Additional information about the eligibility criteria for this trial is presented in Supplementary Table S1.

Kidney Biopsy Procurement and Processing

All participants of the RAIN trial underwent a renal biopsy prior to randomization. The interventionalist procured renal tissue cores during the procedure in a sterile manner. A 2 mm portion of the specimen, designated for molecular studies, was placed directly into green-labeled, white-capped microcentrifuge tubes containing RNALater and stored at −20 °C. The remaining renal tissue was sent for histologic evaluation. Before shipping, the microcentrifuge tubes were placed in biohazard specimen bags, into a 95 kPA pressure-tested container, and sealed in a styrofoam box containing dry ice. Samples were shipped overnight to the Michigan Kidney Translational Core Laboratory at the University of Michigan, where they were stored in batches for transcriptional profiling.

Renal Pathology Studies

A novel histologic scoring system created by Agnes Fogo, an expert renal pathologist, was used to score each renal biopsy.[9] Each standard biopsy was reviewed under light microscopy and scored by 2 renal pathologists. In the months preceding the opening of the RAIN trial, both pathologists trained on deidentified renal slides from a stored collection (non-RAIN patients) at Tufts Medical Center using interactive digital imaging. The training was required to address concerns about the scoring tool and generate an agreement score between reviewers. The pathology slides lacked identifiers. Pathologists were blinded to baseline characteristics and clinical outcomes. Congo red stain was assessed under light microscopy for amorphous deposits, demonstrating "apple green" birefringence under polarized light. AL subtype was verified by immunofluorescence or immunohistochemical staining for kappa and lambda and, if required, by laser microdissection mass spectrometry. Periodic acid-Schiff, Jones methenamine silver stain, and Klatskin trichrome were preferentially used for scoring purposes. An adequate renal sample required the presence of a minimum of 5 glomeruli. The number of glomeruli (including those that were sclerosed and/or fragmented) and the distribution of the biopsy (i.e., cortex and/or medulla) were recorded. The medulla was defined as such if it was without cortical tubules or glomeruli.

AS

Each patient's biopsy was evaluated for distribution (mesangial, capillary wall, interstitial, and vascular) and extent of amyloid deposition (0 = absent; 1+ = minimal, <25%; 2+ = moderate, 25%–50%; and 3+ = severe, >50%) with an average score assigned for each anatomical compartment based on overall involvement. The sum of the average mesangial, capillary, interstitial, and vascular scores generated a single overall AS for each patient (maximum score of 12) (Figure 1a). There was amyloid distribution agreement if scores within subcategories (mesangial, capillary, interstitial, vascular) and final AS were within +/− 1 point of each other, assuming the absence of a negative (0) score.

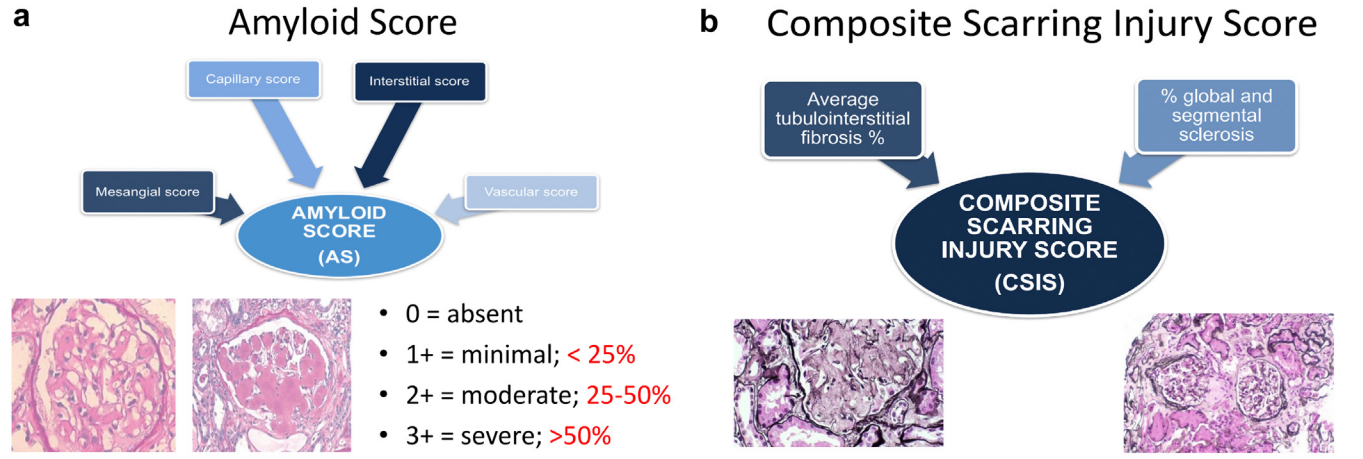

Figure 1. (a) Components of amyloid score. Diagram demonstrating the composition of the amyloid score (AS) made up of the sum of the average mesangial, capillary, interstitial, and vascular scores (maximum score of 12). (b) Components of composite scarring injury score: Diagram demonstrating the composition of the composite scarring injury score (CSIS) made up of the sum of the average percentage of global sclerosis and percentage of tubulointerstitial fibrosis (maximum score of 200).

Composite Scarring Injury Score (CSIS)

The number of glomeruli under light microscopy was noted, and the percent of global sclerosis was calculated (sclerosed glomeruli/total glomeruli) and recorded as a percentage. The degree of TI fibrosis was estimated in each high-power cortical field, and the average percent to the nearest 10% (if <5%, a score of 5% was assigned) was calculated from all cortical fields. The sum of the percentage of global sclerosis and the percentage of TI fibrosis generated a CSIS. There was fibrosis score agreement if scores were within +/− 20% of each other (e.g., scores 60%, 70%, and 80% would be in agreement with an average of 70%) (Figure 1b).

Transcriptional Profiling

The University of Michigan received 9 kidney biopsy cores stored in RNALater by ThermoFisher (cat# AM7020) and delivered to the Kretzler Laboratory. The biopsy was manually dissected under a stereomicroscope using 2 dissection needle holders into their glomerular and tubular interstitial compartments for bulk tissue-specific mRNA sequencing. The separate tissue types were stored in RNALater at −20 °C until RNA isolation. RNA was extracted using the Allprep DNA/RNA Micro Kit (cat# 80284) by Qiagen and eluted in RNAase-free water. The quantity and quality of the RNA were analyzed using a Bioanalyzer 2100 from Agilent. RNA was stored at −80 °C until used for RNAseq processing. cDNA was generated using SMART-Seq v4 Ultra Low Input RNA Kit for Sequencing (cat# 634888) from Takara, and the library was generated using the Low Input Library Prep Kit from Illumina. The University of Michigan DNA Sequencing Core Facility performed cDNA and next-generation sequencing library synthesis. Next-generation sequencing library quantity and quality were assessed using a TapeStation from Agilent. Sequencing was performed on a NextSeq 500/550 from Illumina. This approach has been successfully used to generate high-quality transcriptomic data.[10]

Quality Control

Fastq reads were mapped to the human genome (GRCh38.86) and underwent an iterative quality control, including read-level, mapping-based, and dataset-level metrics. The detailed procedure is described elsewhere.[11] In short, the mapped reads were examined for distribution across exons, introns, untranslated region, and intergenic regions using Picard Tools (https://broadinstitute.github.io/picard/). Gene level expression quantification was performed using HTSeq. The resultant count data were normalized with voom[12] to a log2 counts-per-million (logCPM) scale. Principal component analysis and hierarchical clustering were used to identify and remove samples with abnormal expression profiles due to technical issues, and the mapping statistics were obtained from STAR.

Cluster Analysis

To determine patient groupings, hierarchical cluster analysis was conducted using the R pvclust package[13] and Ward's minimum variance linkage with 500-fold bootstrap sampling. The obtained patient clusters were verified to be robust with several other methods (data not shown). To identify the biological differences between the clusters, we performed differential gene expression between the cluster groups.

Differentially Expressed Genes

Differential gene expression was carried out using the limma[14] package in R, based on the voom normalized and log2 transformed CPM expression values. Genes were significantly regulated at a false discovery rate of 0.05.

Gene Enrichment and Ingenuity Pathway Analyses

Gene enrichment analysis was conducted using g:profiler[15] and default parameters to identify biological concepts enriched in a selected list of genes. Pathway enrichment was conducted with Ingenuity Pathway Analysis (QIAGEN Inc., https://digitalinsights.qiagen.com/IPA). Selected pathways from the top 20 pathways identified at $P < 0.05$ are shown and listed in order of significance.

Comparator Cohorts

Ninety-two glomerular and 113 tubular bulk RNAseq expression profiles of patients with FSGS and 8 (glomerular) and 10 (tubular) living donor samples were obtained from the Nephrotic Syndrome Study Network and used as comparators in this study. Living donors are healthy individuals selected as kidney transplant donors. Nine adult patients with FSGS were subselected based on comparable eGFR and utilized in this comparative analysis. The Nephrotic Syndrome Study Network bulk RNAseq data were generated using the same QC and processing pipeline as the RAIN RNAseq data.

Statistics

Inter-Observer Agreement Calculation for Histologic Scoring

Inter-observer agreement calculations were performed using results from histologic scoring on training slides. For the AS and its 4 components, cross-tabulations and Spearman's rank correlation coefficient were calculated to measure the strength of agreement between the 2 pathologists. For CSIS and its 2 components, scatterplots and Pearson's correlation coefficient were calculated to measure the strength of agreement between the 2 pathologists. The inter-observer agreement calculations resulted in a Pearson's correlation score of 0.94 for the AS and a Spearman's correlation score using cross-tabulations of 0.86. Both scores were deemed acceptable for progressing with the validation set using RAIN biopsy samples.

Statistical Analysis and Correlation Analysis

Prism 6 for Mac OS X (GraphPad *et al.*) was used for statistical analysis. An unpaired *t* test was used to perform the group differences between the AS and CSIS scores between the clusters. Voom transformed bulk RNAseq expression on log2 scale was used to test for correlation between high variable gene sets and histologic (components of the AS and CSIS scores) and clinical variables (creatinine, eGFR, 24-h proteinuria, serum-free light chains, etc.). The Pearson correlation coefficients were determined for a 95% confidence interval; results were considered statistically significant when $P < 0.05$.

RESULTS

The baseline clinical characteristics of patients participating in the RAIN trial are presented in Supplementary Table S2.

Histologic Scores

The AS and CSIS for each participant are listed in Table 1. The median AS was 5.75 (maximum score is 12; range 3.5–9.00). The median CSIS was 19.3 (maximum score is 200; range 5–62). There was no pattern to suggest an apparent correlation between AS, CSIS, and renal outcome because there were too few events. The change in proteinuria among study participants over time is presented in Supplementary Figure S2. There was no association between AS and light chain isotype or serum light chain level, as most patients had normal or suppressed light chain levels.

Transcriptional Profiling

Cluster Analysis

Two distinct patient clusters (G1 and G2) within the tubular and glomerular gene expression sets

Table 1. Histologic scores and renal response

Patient ID	NEOD001 (Y/N)	doses	Initial 24h UTP (mg)	EOS 24h UTP (mg)	AS (0–12)	CSIS (0–200)	Renal response
1	Y	10	3645	3672	6.5	13.4	N
2	N	N/A	6123	5076	6.0	41.0	N
3	Y	6	17032	8348	9.0	62.1	Y
4	N	N/A	5810	4268	4.5	19.1	N
5	N	N/A	1610	Not available	5.5	15.9	Not evaluable
6	Y	1	4023	Not available	3.5	5.0	Not evaluable
7	N	N/A	3367		6.0	19.5	Y
8	N	N/A	9339	Not available	4.5	42.5	Not evaluable
9	Y	1	3426	Not available	3.5	27.0	Not evaluable

AS, amyloid score; CSIS, composite scarring injury score; EOS, end-of-study; ID, identification; N/A, not applicable; UTP, urinary total protein.

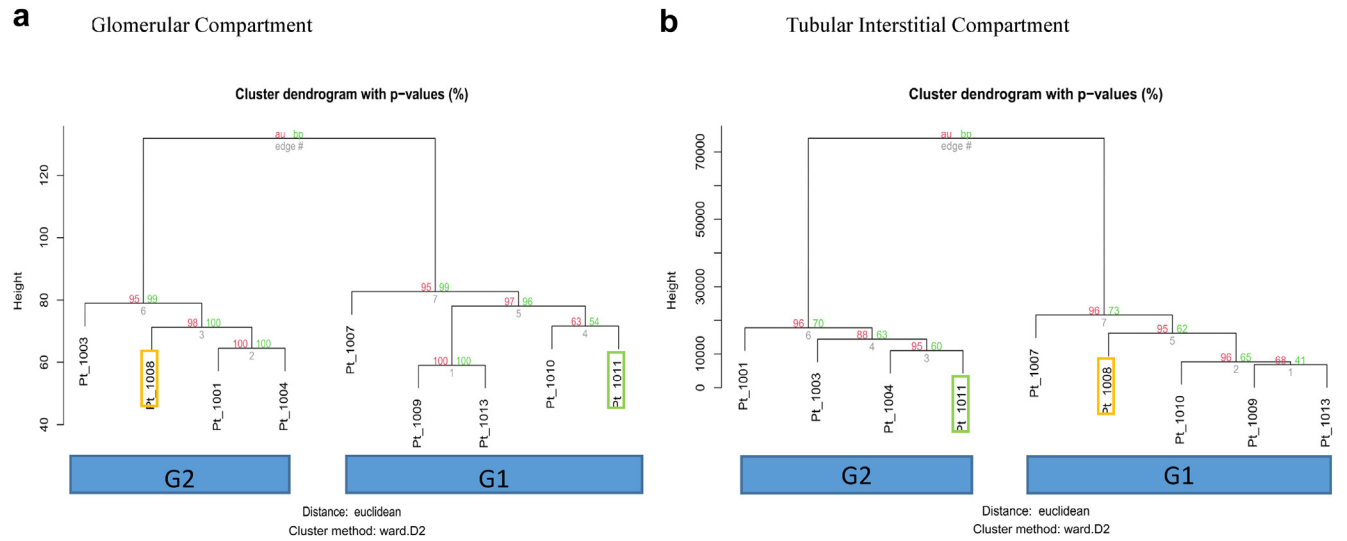

Figure 2. Cluster analysis: unsupervised hierarchical clustering of the glomerular (a) and tubular (b) gene expression identifies 2 broadly consistent clusters (G1/G2). The cluster assignment is consistent in the 2 compartments except for patients 1008 (orange) and 1011 (green).

(Figure 2a and b) were identified with distinct separations in the TI compartment. Cluster composition of G1 and G2 mainly was consistent between glomerular and TI compartments, with patients 1008 and 1011 changing places. Patients 1008 and 1011 were the only patients with a measurable monoclonal protein greater than 1 g/dl (5.6 g/dl and 3.5 g/dl, respectively). Otherwise, no other characteristics or factors were unique to these 2 patients. Of note, treatment history, hematologic status, disease isotype, degree of proteinuria, and eGFR were not statistically significant between G1 and G2 in either compartment. Only 1 patient in each cluster had a documented renal response. The histopathologic features significantly differed between G1 and G2; the median AS was significantly higher in G2 versus G1 in the tubular compartment (6.5 vs. 4.5; $P = 0.0290$). The increase in AS in G2 was driven almost entirely by an increase in mesangial and capillary wall amyloid deposition. The median CSIS was higher in G2 versus G1 in the glomerular compartment, which was nearing significance (28.4 vs. 19.5; $P = 0.0536$).

Serum lambda light chain levels correlated with 746 genes in the TI compartment and 279 in the glomerular compartment, with a false discovery rate threshold of 0.05 (Supplementary Figure S3). The CSIS score correlated to 97 genes in the tubular interstitial compartment. None of the other histologic and clinical variables (proteinuria, kappa light chains, and eGFR) correlated significantly with this high-variance gene set.

Differential Expression

There were more differentiated genes between G1 and G2 in the glomerular compartment than in the TI compartment (815 vs. 371) (Supplementary Figure S4). The most significantly differentiated genes between G1 and G2 in the glomerular compartment were associated with various molecular functions, including NADPH-dependent deiodination (e.g., *IYD*), transportation of molecules across cell membranes (e.g., *ABCC6*), phosphate homeostasis (e.g., *SLC34A1*), proteins involved in basement membrane anchoring (e.g., *FREM2*) and RNA binding activity (*RBM47*), among many others. There was significant enrichment in G1 versus G2 among gene ontology classes which included "transmembrane transporter activity," "small molecule binding," "extracellular exosome/organelle/vesicle," and multiple catabolic/metabolic processes. Upregulated KEGG pathways included "metabolic pathways," "carbon metabolism," and "valine, leucine, and isoleucine degradation" (Figure 3a and b). In Figure 4a and b, we provide a summary of the significant genes, upstream regulators, and gene functions between G1 and G2 resulting from the limma differentially expressed genes analysis divided into the tubular and glomerular compartments with an adjusted P-value <0.05. Glomeruli showed activation of fibrotic pathways accompanied by a reduction in metabolic processes, including gluconeogenesis, lipid transport, and xenobiotics. An increase in canonical signaling of LPS/IL-1–mediated inhibition of RXR function drives increased IL1 and TNF release from macrophages. Transcriptomic evidence of TNF activation was also noted in the TI. Other enriched ingenuity canonical pathways to note in the TI included "coagulation system," "GADD45 signaling," "Wnt/Ca+ pathway," and "intrinsic prothrombin activation pathway," among others. Notably, genes such as *BRCA* and *CDKN1A* were enriched between G1 and G2, both of which have been associated with molecular mechanisms underlying certain neoplasms (Supplementary Table S3).

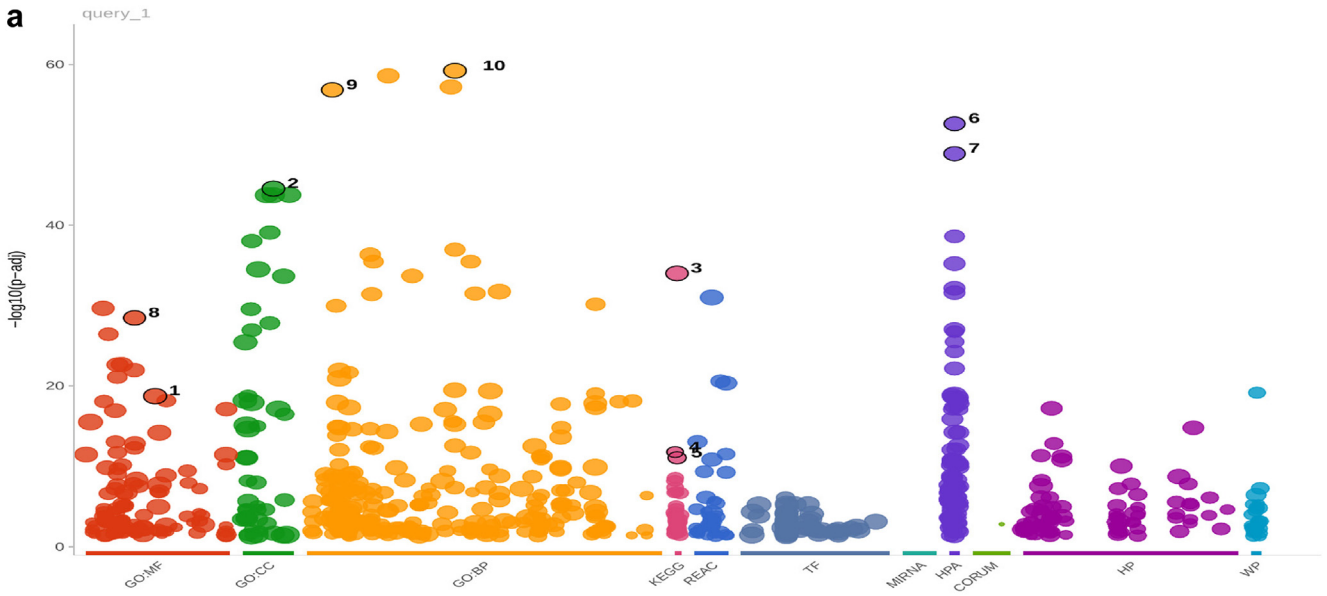

id	source	term_id	term_name	term_size	p_value
1	GO:MF	GO:0036094	small molecule binding	2584	1.8e−19
2	GO:CC	GO:0070062	extracellular exosome	2109	2.8e−45
3	KEGG	KEGG:01100	Metabolic pathways	1532	9.7e−35
4	KEGG	KEGG:00280	Valine, leucine and isoleucine degradation	48	1.6e−12
5	KEGG	KEGG:01200	Carbon metabolism	115	8.5e−12
6	HPA	HPA:0271142	kidney; proximal tubules (cell body)[...Medium]	566	2.3e−53
7	HPA	HPA:0271141	kidney; proximal tubules (cell body)[...Low]	727	1.2e−49
8	GO:MF	GO:0022857	transmembrane transporter activity	1121	3.4e−29
9	GO:BP	GO:0006082	organic acid metabolic process	979	1.4e−57
10	GO:BP	GO:0044281	small molecule metabolic process	1865	6.0e−60

g:Profiler (biit.cs.ut.ee/gprofiler)

Figure 3. Enriched gene profiles in the glomerular compartment between G1 and G2: functional enrichment of the genes significantly regulated between G1 and G2 in the glomerular compartment with g:Profiler. (a) Selected enrichment terms are detailed in the table. (Continued)

When comparing signatures between healthy controls and amyloidosis patients, ingenuity pathway analysis identified unique activation signatures in the glomeruli and tubules. In the glomeruli, there was increased signaling of TNF, NFKB, IL33, IL-8, and IL15, consistent with an important inflammatory response. There was also an enrichment in migration, adhesion, and integrin signaling pathways with a coexisting activated immune system. A predicted increase in canonical PI3K/Akt signaling was also noted. Tubules showed increased activation of transcriptional regulators TP53, TP73, integrin signaling, and increased cytokine signaling of IFNG, TGFb1, and VEGF. There was also a predicted activation of major canonical pathways, including B cell receptor signaling, PI3K/AKT, and ephrin receptor signaling (Figure 5a and b). Some gene regulators of cellular proliferation, such as *ABL1*, *BCL2*, and *AKT1*, were found to be enriched in the amyloid group.

After batch correction with ComBat,[16] a cluster analysis was conducted using the 9 subselected FSGS and the 9 amyloid samples (Supplementary Figure S5A and B). The FSGS samples clustered mostly with G2 in the glomerulus but did not demonstrate clear subclusters. Except for 1 patient, the G1 clustered with the healthy controls. In the TI, the G1 group clustered primarily with patients with FSGS and secondarily with healthy controls, whereas all except 1 from the G2 group clustered separately with patients with FSGS.

DISCUSSION

Patients with renal AL amyloidosis have been grouped under a single diagnosis based on histologic features; however, they represent a heterogeneous group that has significant variability in symptoms, rate of progression, and response to therapy. A primary challenge to improving clinical outcomes in renal amyloidosis is the inability to identify patients who are at high risk for renal deterioration early in their disease course before irreversible damage can ensue. eGFR and proteinuria, although conventional predictors of chronic kidney disease progression, do not reflect the mechanisms underlying the decline in kidney function, and thus, they remain poor predictors of chronic kidney disease progression in AL. Unfortunately, our current

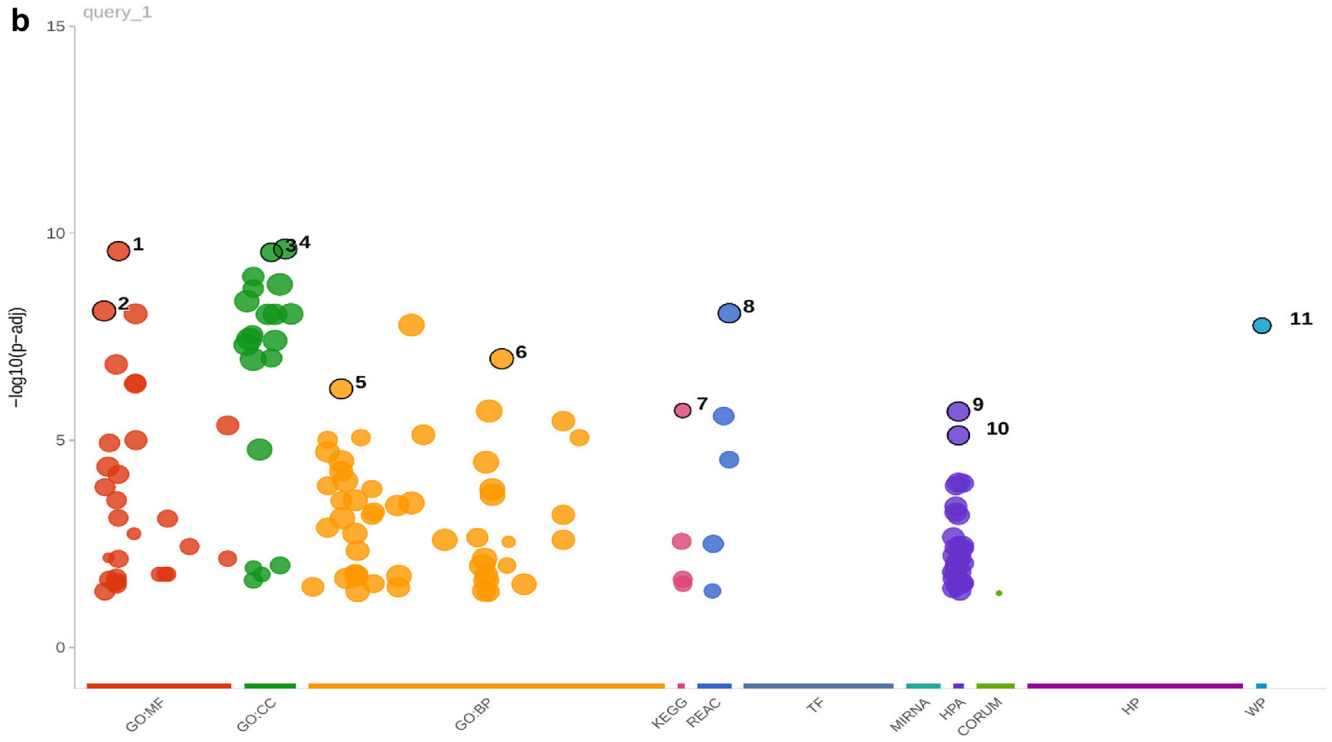

id	source	term_id	term_name	term_size	p_value
1	GO:MF	GO:0015318	inorganic molecular entity transmembrane transporter activity	680	2.7e−10
2	GO:MF	GO:0005215	transporter activity	1231	7.6e−09
3	GO:CC	GO:0045177	apical part of cell	449	2.9e−10
4	GO:CC	GO:0098590	plasma membrane region	1292	2.4e−10
5	GO:BP	GO:0006811	monoatomic ion transport	1274	5.7e−07
6	GO:BP	GO:0055085	transmembrane transport	1558	1.1e−07
7	KEGG	KEGG:04966	Collecting duct acid secretion	27	1.9e−06
8	REAC	REAC:R−HSA−382551	Transport of small molecules	720	8.6e−09
9	HPA	HPA:0271141	kidney; proximal tubules (cell body)[...Low]	727	2.0e−06
10	HPA	HPA:0271142	kidney; proximal tubules (cell body)[...Medium]	566	7.6e−06
11	WP	WP:WP4917	Proximal tubule transport	57	1.7e−08

g:Profiler (biit.cs.ut.ee/gprofiler)

Figure 3. (Continued) (b) Functional enrichment of the genes significantly regulated between G1 and G2 in the tubular compartment with g:Profiler. Selected enrichment terms are detailed in the table.

understanding of renal amyloidosis stems from retrospective studies subject to confounding information, difficulties establishing temporal relationships, and the inability to determine causation.

There are very little published data related to transcriptional profiling in AL amyloidosis. Much of the genomic profiling has been on the clonal plasma cells or cardiomyocytes.[17–19] This is the first study looking at transcriptional profiling of renal tissue. The RAIN trial was the first study dedicated exclusively to renal amyloidosis. We leveraged the prospective design of this study by incorporating ancillary studies to identify molecular signatures unique to AL nephropathy. We then used bioinformatic strategies to correlate molecular and histologic data with clinical parameters to uncover regulatory pathways that may play an essential role in the pathogenesis of this disease. The ingenuity pathways reported in this study are in keeping with what one would expect with tubular interstitial fibrosis, indicating that the tissue response to amyloid deposition induces an inflammatory and innate immune response similar to those seen in other chronic kidney diseases. Upregulated proteins included inflammatory cytokines such as TNF, IL33, IL15, and IL-8. Major upregulated canonical pathways included B cell receptor signaling, PI3K/AKT, and ephrin receptor signaling.

This study's unique and unexpected observation was the discovery of 2 distinct patient clusters (G1 and G2) based on gene expression signatures within both the tubular and glomerular gene sets. Patients within the G2 cluster had significantly more amyloid deposition in the tubular interstitial compartment, as

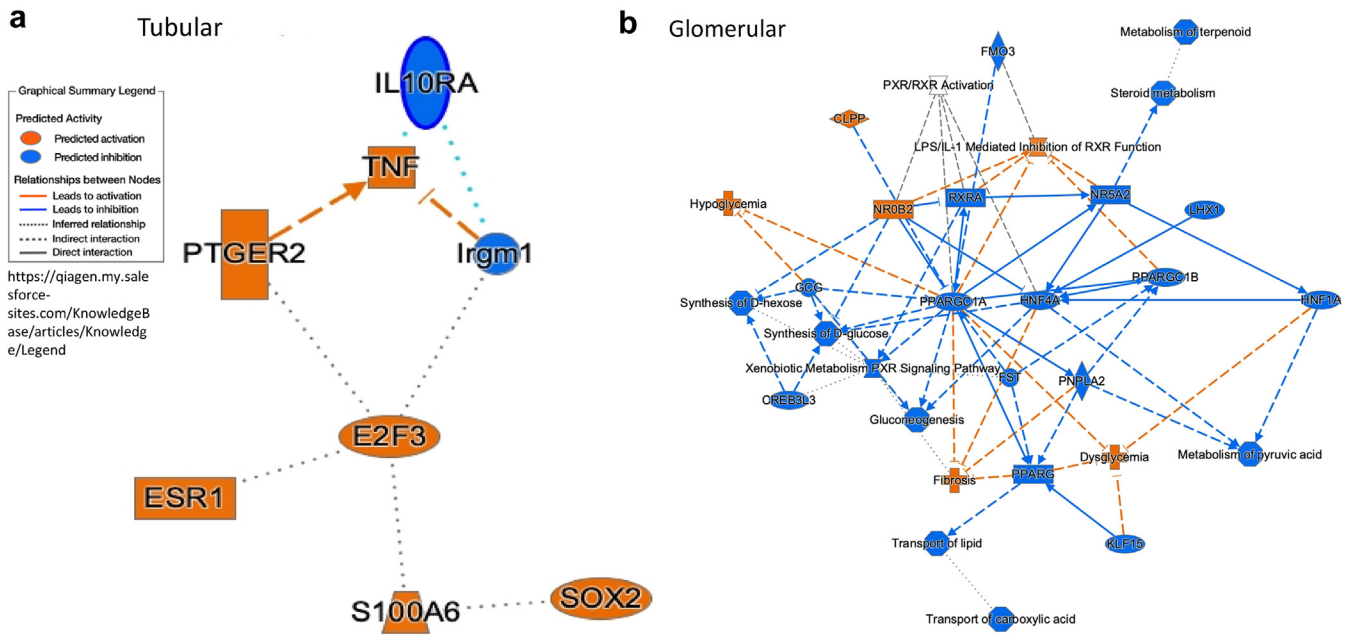

Figure 4. Enriched gene profiles G1 versus G2. Ingenuity pathway analysis upstream regulator analysis of significantly regulated transcripts between G2 and G1. (a) shows the tubular, and (b) the glomerular compartment. All input genes are significant at <0.05 after multiple testing corrections.

evidenced by the higher AS via microscopic evaluation. No other demographic or disease variables significantly differed between the 2 clusters. However, it is unclear if other clinical factors such as diabetes, hypertension, or obesity, could explain the distinctive groupings. The most differentially regulated genes between these 2 patient groups at the molecular level were associated with proteins involved in transportation across cell membranes and proteins related to basement membrane anchoring. G2 contained more differentiated genes related to inflammation, such as TNF, IFNG, IL33, and VEGFA, resulting in an increase in canonical PI3K/Akt signaling and innate immune responses compared to G1. Pathways related to fibrosis were also enriched in G2. Unfortunately, we could not correlate G1 or G2 to renal survival due to short follow-up time and too few renal events.

Interestingly, when comparing gene expression profiles between patients with renal amyloidosis and healthy controls, many upregulated pathways involved cancer-related molecular mechanisms such as Her2, ABL1, BCL2, p53, B cell receptor, and PI3K/AKT

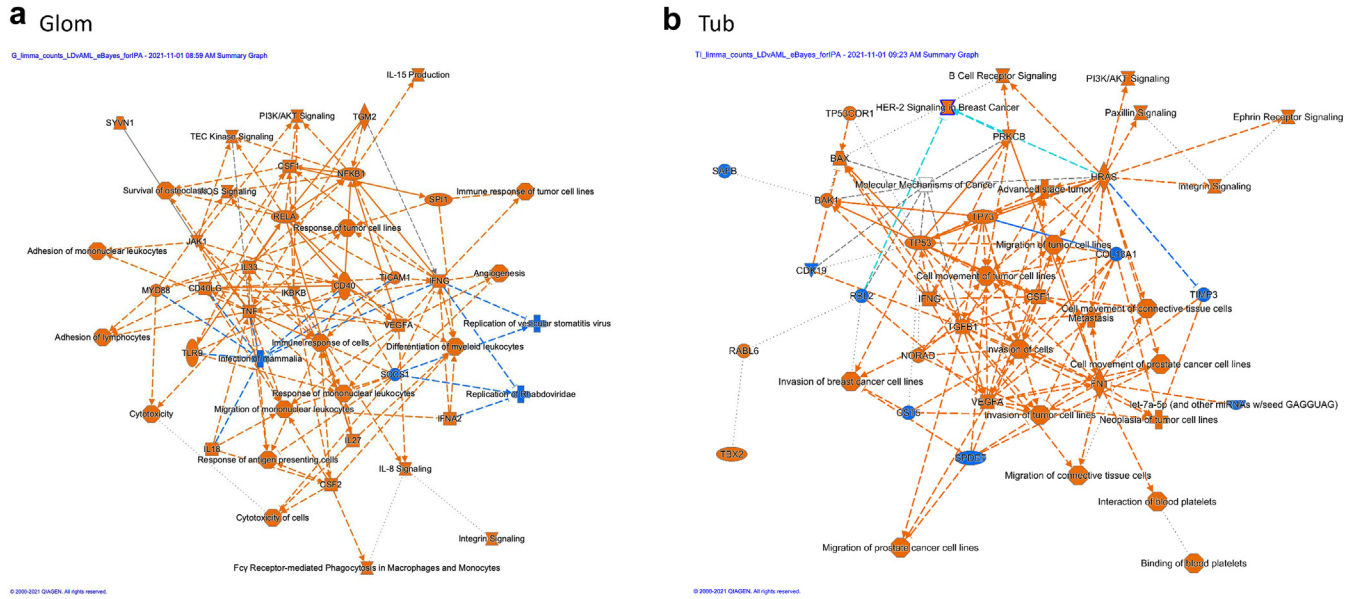

Figure 5. (a and b) Enriched gene profiles in the tubular and glomerular compartments between living donor and amyloidosis samples.

signaling. The PI3K/Akt pathway has been linked to the presence of amyloid-β neurofibrillary tangles, as seen in Alzheimer's disease.[20] In this disease, the accumulated Aβ oligomers prevent PI3K/Akt signaling, resulting in increased protein kinase activity in neurons, increased apoptosis, and diminished cell survival.[21]

In this study, it is unclear whether the increased signaling of the PI3K/Akt pathway in patients with AL amyloidosis plays a pivotal role in amyloid deposition or occurs in response to amyloid fibril–induced inflammation within renal tissue. PI3K/Akt pathway plays several vital roles in phagocytosis and the macrophage response to pathogens.[22] There are 2 macrophage phenotypes depending on Akt isoform: M1 and M2. The former is proinflammatory with enhanced production of IL-6 and TNF-alpha, whereas the latter has antiinflammatory properties.[23,24] In this study, it remains to be seen what isotype of Akt is overexpressed; thus, more data is required to address this critical question. Ideally, comparing expression levels of PI3K/Akt at various time points of the disease (e.g., at diagnosis, upon treatment completion, and at the time of organ response) would be ideal for forming a hypothesis about this pathway in AL amyloidosis. NEOD001 and CAEL101, both novel monoclonal antibodies that target misfolded light chains, are currently being investigated in phase III clinical trials in AL amyloidosis (NCT04512235, NCT04504825, NCT04973137). Their mechanism of action relies heavily on the phagocytic destruction and subsequent clearance of amyloid deposits. Expanding on the potential impact of the PI3K/Akt pathway on phagocytosis or macrophage activation in AL amyloidosis would be valuable, especially with the notion that pharmacological inhibitors of this pathway already exist. The inhibition of PI3K/Akt signaling in chronic kidney disease may reduce extracellular matrix deposition in the renal interstitium, preventing progressive nephropathy development.

Another unexpected finding was that of all the clinical variables analyzed. the lambda light chain levels correlated significantly with genes in the glomerular and TI compartments. These significant genes are related to various functions, including the production of the Ig lambda light chain variable region, the regulation of cell adhesion, cytoskeleton organization, and cell migration, among many others. It remains unclear if this finding is related to a clonal process as is well established in AL amyloidosis, a disease in which two-thirds of patients present with lambda-isotype, or whether it can be attributed to nonspecific inflammatory changes within the kidney. Next-generation sequencing at the single-cell level may shed more light on this question.

The most evident weakness of this study was the smaller than anticipated sample size due to the premature closure of the RAIN trial, a decision made by the developers of NEOD001 based on a futility analysis of the phase 3 VITAL study (NCT02632786) utilizing NEOD001 in previously treated patients with cardiac amyloid. This resulted in several missed opportunities, including our inability to validate a novel histologic scoring system. Although this scoring system aimed to derive prognostic information by standardizing measurements of amyloid deposition and renal injury, we could not correctly substantiate it on a large scale. Irrespective of this fact, we believe that this scoring system can be of significant benefit and should be validated in the future. If adopted globally, it has the potential to eliminate ambiguities and inconsistencies and allow for the standardization and formal comparison of biopsy reports across all institutions and therapeutic clinical trials. Another shortcoming is the need for more available data pertaining to comorbidities, which may or may not have influenced the clustering analysis.

The few trial participants and short follow-up period also meant a trivial number of renal events in this study, making it impossible to correlate any observed findings to renal outcomes. Any observations from this study may have been due to chance, and thus, any inferences from this study must be made with caution.

Despite these shortcomings, the RAIN trial still represents an accomplishment in the field of AL amyloidosis; it demonstrated that it was possible to successfully collect adequate fresh renal tissue from patients and perform complex transcriptional analysis. Furthermore, despite the small sample size, we could effectively identify 2 distinct groups of patients based on molecular signatures correlated with the amyloid burden. This data were robust enough to evaluate algorithms and data perturbation, making this a compelling proof-of-concept that can serve as a steppingstone for future molecular studies. These data are tangible and promising. By identifying distinct subgroups in this renal population, we can better risk-stratify earlier in the course of the disease and be able to therapeutically intervene based on molecular targets in the future. A large cohort of patients with renal amyloid would be necessary to help categorize tissue response to amyloid deposits at a single cell resolution and by kidney cell type. Understanding cellular responses at a molecular level could provide novel therapeutic targets to mitigate renal injury and improve patient outcomes.

APPENDIX

List of Members of the Nephrotic Syndrome Study Network (NEPTUNE), NEPTUNE Collaborating Sites

Atrium Health Levine Children's Hospital, Charlotte, SC: Susan Massengill, Layla Lo; Cleveland Clinic, Cleveland, OH: Katherine Dell, John O'Toole, John Sedor, Blair Martin; Children's Hospital, Los Angeles, CA: Ian Macumber, Silpa Sharma; Children's Mercy Hospital, Kansas City, MO: Tarak Srivastava, Kelsey Markus; Cohen Children's Hospital, New Hyde Park, NY: Christine Sethna, Suzanne Vento; Columbia University, New York, NY: Pietro Canetta; Duke University Medical Center, Durham, NC: Opeyemi Olabisi, Rasheed Gbadegesin, Maurice Smith; Emory University, Atlanta, GA: Laurence Greenbaum, Chia-shi Wang, Emily Yun; The Lundquist Institute, Torrance, CA: Sharon Adler, Janine LaPage; John H Stroger Cook County Hospital, Chicago, IL: Amatur Amarah, Mathew Itteera; Johns Hopkins Medicine, Baltimore, MD: Meredith Atkinson, Miahje Williams; Mayo Clinic, Rochester, MN: John Lieske, Marie Hogan, Fernando Fervenza; Medical University of South Carolina, Charleston, SC: David Selewski, Cheryl Alston; Montefiore Medical Center, Bronx, NY: Kim Reidy, Michael Ross, Frederick Kaskel, Patricia Flynn; New York University Medical Center, New York, NY: Laura Malaga-Dieguez, Olga Zhdanova, Laura Jane Pehrson, Melanie Miranda; The Ohio State University College of Medicine, Columbus, OH: Salem Almaani, Laci Roberts Stanford University, Stanford, CA: Richard Lafayette, Shiktij Dave; Temple University, Philadelphia, PA: Iris Lee; Texas Children's Hospital at Baylor College of Medicine, Houston, TX: Shweta Shah, Sadaf Batla; University Health Network Toronto: Heather Reich, Michelle Hladunewich, Paul Ling, Martin Romano; University of California at San Francisco, San Francisco, CA: Paul Brakeman; University of Colorado Anschutz Medical Campus, Aurora, CO: James Dylewski Nathan Rogers; University of Kansas Medical Center, Kansas City, KS: Ellen McCarthy, Catherine Creed; University of Miami, Miami, FL: Alessia Fornoni, Miguel Bandes; University of Michigan, Ann Arbor, MI: Matthias Kretzler, Laura Mariani, Zubin Modi, A Williams, Roxy Ni; University of Minnesota, Minneapolis, MN: Patrick Nachman, Michelle Rheault, Amy Kowalski, Nicolas Rauwolf; University of North Carolina, Chapel Hill, NC: Vimal Derebail, Keisha Gibson, Anne Froment, Sara Kelley; University of Pennsylvania, Philadelphia, PA: Lawrence Holzman, Kevin Meyers, Krishna Kallem, Aliya Edwards; University of Texas San Antonio, San Antonio, TX: Samin Sharma; University of Texas Southwestern, Dallas, TX: Elizabeth Roehm, Kamalanathan Sambandam, Elizabeth Brown, Jamie Hellewege; University of Washington, Seattle, WA: Ashley Jefferson, Sangeeta Hingorani, Katherine Tuttle, Linda Manahan , Emily Pao, Kelli Kuykendall; Wake Forest University Baptist Health, Winston-Salem, NC: Jen Jar Lin; Washington University in St. Louis, St. Louis, MO: Vikas Dharnidharka; Data Analysis and Coordinating Center: University of Michigan: Matthias Kretzler, Brenda Gillespie, Laura Mariani, Zubin Modi, Eloise Salmon, Howard Trachtman, Tina Mainieri, Gabrielle Alter, Michael Arbit, Hailey Desmond, Sean Eddy, Damian Fermin, Wenjun Ju, Maria Larkina, Chrysta Lienczewski, Rebecca Scherr, Jonathan Troost, Amanda Williams, Yan Zhai; Arbor Collaborative for Health: Colleen Kincaid, Shengqian Li, Shannon Li; Cleveland Clinic: Crystal Gadegbeku, Duke University: Laura Barisoni; John Sedor, Harvard University: Matthew G Sampson; Northwestern University: Abigail Smith; University of Pennsylvania: Lawrence Holzman, Jarcy Zee; Digital Pathology Committee: Carmen Avila-Casado (University Health Network), Serena Bagnasco (Johns Hopkins University), Lihong Bu (Mayo Clinic), Shelley Caltharp (Emory University), Clarissa Cassol (Arkana), Dawit Demeke (University of Michigan), Brenda Gillespie (University of Michigan), Jared Hassler (Temple University), Leal Herlitz (Cleveland Clinic), Stephen Hewitt (National Cancer Institute), Jeff Hodgin (University of Michigan), Danni Holanda (Arkana), Neeraja Kambham (Stanford University), Kevin Lemley, Laura Mariani (University of Michigan), Nidia Messias (Washington University), Alexei Mikhailov (Wake Forest), Vanessa Moreno (University of North Carolina), Behzad Najafian (University of Washington), Matthew Palmer (University of Pennsylvania), Avi Rosenberg (Johns Hopkins University), Virginie Royal (University of Montreal), Miroslav Sekulik (Columbia University), Barry Stokes (Columbia University), David Thomas (Duke University), Ming Wu (University of New York), Michifumi Yamashita (Cedar Sinai), Hong Yin (Emory University), Jarcy Zee (University of Pennsylvania), Yiqin Zuo (University of Miami). Co-Chairs: Laura Barisoni (Duke University) and Cynthia Nast (Cedar Sinai).

DISCLOSURE

All the authors declared no competing interests.

ACKNOWLEDGMENTS

We want to thank the George M. O'Brien Michigan Kidney Translational Core Center team: Felix Eichinger, Viji Nair, Abhijit S. Naik MD, and Dr. Matthias Kretzler for performing the transcriptional profiling of the renal samples and helping in the interpretation of the data. We thank Dr. Agnes Fogo for allowing us to utilize her histologic scoring method. We thank Dr. Samih Nasr and Dr. Agnes Fogo for scoring all the renal biopsies. We want to thank the Nephrotic Syndrome Study Network for allowing us to use

existing renal expression profiles. We would like to thank the Multiple Myeloma Research Foundation for funding this project through the 2018 MMRF Fellowship grant.

The Nephrotic Syndrome Study Network (NEPTUNE) is part of the Rare Diseases Clinical Research Network (RDCRN), which is funded by the National Institutes of Health (NIH) and led by the National Center for Advancing Translational Sciences (NCATS) through its Division of Rare Diseases Research Innovation (DRDRI). NEPTUNE is funded under grant number U54DK083912 as a collaboration between NCATS and the National Institute of Diabetes and Digestive and Kidney Diseases (NIDDK). Additional funding and/or programmatic support is provided by the University of Michigan, NephCure, Alport Syndrome Foundation, and the Halpin Foundation. RDCRN consortia are supported by the RDCRN Data Management and Coordinating Center (DMCC), funded by NCATS and the National Institute of Neurological Disorders and Stroke (NINDS) under U2CTR002818.

This work was supported by grant U54-DK137314 from the George M. O'Brien National Resource Center at the University of Michigan and the National Institute of Diabetes and Digestive and Kidney Diseases (NIDDK)

ASN acknowledges support from the George M. O'Brien Michigan Kidney National Resource Center, funded by NIH/NIDDK grant U54DK137314, the First Pathway Award, Michigan Institute of Clinical Health Research UL1TR002240, Department of Internal Medicine, and the National Institute of Health K23 DK 125529.

DATA AVAILABILITY STATEMENT

The expression matrix of this data and the corresponding fastq files will be made available in GEO.

SUPPLEMENTARY MATERIAL

Supplementary File (PDF)

Figure S1. RAIN study design.

Figure S2. Change in proteinuria.

Figure S3. Gene Expression correlates to histopathological features.

Figure S4. Differentially expressed gene analysis.

Figure S5. Cluster analysis focal segmental glomerulosclerosis/amyloidosis samples.

Table S1. Inclusion/exclusion criteria.

Table S2. Baseline characteristics.

Table S3. Enriched Pathways and genes between G1 and G2 in the tubular compartment.

STROBE Checklist.

REFERENCES

1. Obici L, Perfetti V, Palladini G, Moratti R, Merlini G. Clinical aspects of systemic amyloid diseases. *Biochim Biophys Acta*. 2005;1753:11–22. https://doi.org/10.1016/j.bbapap.2005.08.014
2. Kyle RA, Gertz MA. Primary systemic amyloidosis: clinical and laboratory features in 474 cases. *Semin Hematol*. 1995;32:45–59.
3. Palladini G, Dispenzieri A, Gertz MA, et al. New criteria for response to treatment in immunoglobulin light chain amyloidosis based on free light chain measurement and cardiac biomarkers: impact on survival outcomes. *J Clin Oncol*. 2012;30:4541–4549. https://doi.org/10.1200/JCO.2011.37.7614
4. Palladini G, Hegenbart U, Milani P, et al. A staging system for renal outcome and early markers of renal response to chemotherapy in AL amyloidosis. *Blood*. 2014;124:2325–2332. https://doi.org/10.1182/blood-2014-04-570010
5. Pinney JH, Lachmann HJ, Bansi, et al. Outcome in renal Al amyloidosis after chemotherapy. *J Clin Oncol*. 2011;29:674–681. https://doi.org/10.1200/JCO.2010.30.5235
6. Kumar SK, Dispenzieri A, Lacy MQ, et al. Changes in the serum-free light chain rather than intact monoclonal immunoglobulin levels predict outcomes following therapy in primary amyloidosis. *Am J Hematol*. 2011;86:251–255. https://doi.org/10.1002/ajh.21948
7. Wong SW, Toskic D, Warner M, et al. Primary amyloidosis with renal involvement: outcomes in 77 consecutive patients at a Single Center. *Clin Lymphoma Myeloma Leuk*. 2017;17:759–766. https://doi.org/10.1016/j.clml.2017.06.004
8. Zago W, Renz M, Torres R, et al. NEOD001 specifically binds aggregated light chain infiltrates in multiple organs from patients with AL amyloidosis, and promotes phagocytic clearance of AL aggregates in vitro. *Blood*. 2015;126:3016. https://doi.org/10.1182/blood.V126.23.3016.3016
9. Rubinstein S, Cornell RF, Du L, et al. Novel pathologic scoring tools predict end-stage kidney disease in light chain (AL) amyloidosis. *Amyloid*. 2017;24:205–211. https://doi.org/10.1080/13506129.2017.1360272
10. Mariani LH, Eddy S, AlAkwaa FM, et al. Precision nephrology identified tumor necrosis factor activation variability in minimal change disease and focal segmental glomerulosclerosis. *Kidney Int*. 2023;103:565–579. https://doi.org/10.1016/j.kint.2022.10.023
11. Hong C, Eichinger F, Atta MG, et al. Viral associations with kidney disease diagnosis and altered kidney metatranscriptome by kidney function. *Kidney Int*. 2023;103:218–222. https://doi.org/10.1016/j.kint.2022.11.001
12. Law CW, Chen Y, Shi W, Smyth GK. voom: Precision weights unlock linear model analysis tools for RNA-seq read counts. *Genome Biol*. 2014;15:R29. https://doi.org/10.1186/gb-2014-15-2-r29
13. Winbanks CE, Grimwood L, Gasser A, Darby IA, Hewitson TD, Becker GJ. Role of the phosphatidylinositol 3-kinase and mTOR pathways in the regulation of renal fibroblast function and differentiation. *Int J Biochem Cell Biol*. 2007;39:206–219. https://doi.org/10.1016/j.biocel.2006.08.004
14. Ritchie ME, Phipson B, Wu D, et al. limma powers differential expression analyses for RNA-sequencing and microarray studies. *Nucleic Acids Res*. 2015;43:e47. https://doi.org/10.1093/nar/gkv007
15. Raudvere U, Kolberg L, Kuzmin I, et al. g:Profiler: a web server for functional enrichment analysis and conversions of gene lists. *Nucleic Acids Res*. 2019;47:W191–W198. https://doi.org/10.1093/nar/gkz369

16. Johnson WE, Li C, Rabinovic A. Adjusting batch effects in microarray expression data using empirical Bayes methods. *Biostatistics*. 2007;8:118–127. https://doi.org/10.1093/biostatistics/kxj037

17. Wang Y, Xu L, Liu Y, et al. Transcriptional heterogeneity of clonal plasma cells and immune evasion in immunoglobulin light chain amyloidosis. *Int J Hematol*. 2021;113:231–242. https://doi.org/10.1007/s12185-020-03016-3

18. Kryukov F, Kryukova E, Brozova L, et al. Does AL amyloidosis have a unique genomic profile? Gene expression profiling meta-analysis and literature overview. *Gene*. 2016;591:490–498. https://doi.org/10.1016/j.gene.2016.06.017

19. Shi J, Guan J, Jiang B, et al. Amyloidogenic light chains induce cardiomyocyte contractile dysfunction and apoptosis via a non-canonical p38alpha MAPK pathway. *Proc Natl Acad Sci U S A*. 2010;107:4188–4193. https://doi.org/10.1073/pnas.0912263107

20. Kumar M, Bansal N. Implications of phosphoinositide 3-kinase-Akt (PI3K-Akt) pathway in the pathogenesis of Alzheimer's disease. *Mol Neurobiol*. 2022;59:354–385. https://doi.org/10.1007/s12035-021-02611-7

21. Razani E, Pourbagheri-Sigaroodi A, Safaroghli-Azar A, Zoghi A, Shanaki-Bavarsad M, Bashash D. The PI3K/Akt signaling axis in Alzheimer's disease: a valuable target to stimulate or suppress? *Cell Stress Chaperones*. 2021;26:871–887. https://doi.org/10.1007/s12192-021-01231-3

22. Vergadi E, Ieronymaki E, Lyroni K, Vaporidi K, Tsatsanis C. Akt signaling pathway in macrophage activation and M1/M2 polarization. *J Immunol*. 2017;198:1006–1014. https://doi.org/10.4049/jimmunol.1601515

23. Orecchioni M, Ghosheh Y, Pramod AB, Ley K. Macrophage polarization: different Gene signatures in M1 (LPS+) vs. classically and M2 (LPS−) vs. alternatively activated macrophages. *Front Immunol*. 2019;10:1084. https://doi.org/10.3389/fimmu.2019.01084

24. Stegelmeier AA, van Vloten JP, Mould RC, et al. Myeloid cells during viral infections and inflammation. *Viruses*. 2019;11. https://doi.org/10.3390/v11020168